

Theory of Zn-Enhanced Disorder in GaAs/AlAs Superlattices

C. Wang, Q.-M. Zhang, and J. Bernholc

Department of Physics, North Carolina State University, Raleigh, North Carolina 27695-8202
(Received 17 September 1992)

The microscopic mechanisms for Zn diffusion in GaAs and Zn-induced interdiffusion in GaAs/AlAs superlattices are investigated by *ab initio* molecular dynamics. Among the various proposed mechanisms for Zn diffusion, kick-out by Ga interstitials has the lowest activation energy. Zn in-diffusion generates nonequilibrium group-III interstitials, which are bound to Zn by Coulomb forces. The interstitials follow the Zn diffusion front and disorder the superlattice. The calculated activation energies for these processes are in good agreement with the experimental data.

PACS numbers: 68.35.Fx, 61.70.Wp, 66.30.Jt, 66.30.Ny

Because of its effective lattice match, a variety of growth methods, and potential applications, GaAs/AlAs superlattices have been studied intensively for many years. While the layer structure of the superlattice is stable up to high temperatures ($\sim 900^\circ\text{C}$), it can be destroyed at much lower temperatures ($\sim 500\text{--}600^\circ\text{C}$) through the exchange of Ga and Al atoms during Zn in-diffusion [1]. The exchange between the group-III elements is thus enhanced by several orders of magnitude. The disordering of the layers occurs only in those regions of the material where Zn is present. Afterwards, similar impurity-induced layer disordering has also been found in other III-V superlattices, but the Zn-enhanced interdiffusion in GaAs/AlAs has been studied most extensively. In this Letter we investigate the microscopic mechanism of this effect via *ab initio* molecular dynamics calculations. Apart from its fundamental interest, this phenomenon can be used for selective disordering or patterning in devices, such as solid state lasers and optical waveguides.

Several phenomenological models have been proposed to explain Zn diffusion in III-V semiconductors [2–5]. In the dissociative mechanism, Zn, which is a shallow substitutional acceptor, leaves its site and moves rapidly in the interstitial channel. It becomes substitutional when a group-III vacancy is encountered [2]. Other vacancy-based mechanisms assume that a substitutional Zn and a nearest-neighbor vacancy form a pair that migrates through a series of nearest- or second-nearest-neighbor hops [4,5]. In the kick-out mechanism [3,6] an interstitial Zn joins the group-III sublattice by pushing the host atom away and creating a group-III interstitial. In this Letter we examine the various mechanisms of interdiffusion, searching for the lowest-energy diffusion path for Zn and the exchange paths between Ga and Al. We find that the microscopic mechanism of interdiffusion involves a series of kick-out transformations of Zn and group-III atoms. This mechanism explains naturally the differences between interdiffusion processes with and without Zn, as well as the difference between in- and out-diffusion of Zn. The calculated activation energies are in good agreement with experimental data.

The calculations are performed using the Car-Par-

rinello (CP) methodology [7]. The electrons are described in the local-density approximation and norm-conserving pseudopotentials [8], modified to avoid a Ga “ghost” state [9], were used. For Zn, a soft core pseudopotential, which includes the $3d$ shell in the core, was constructed and tested on bulk ZnTe and ZnSe [10]. Because of the large activation energies for Zn diffusion and cation exchange, a direct *ab initio* molecular dynamics simulation of these processes is not possible at present. Instead, one needs to investigate individual mechanisms and compute their activation energies. The mechanism with the lowest activation energy is the preferred path. The formation energies are computed from total energy calculations, while the migration energies are extracted from total energy differences between the saddle points and the initial states of the diffusing atom or complex, both in a 64-atom supercell. All calculations included plane waves with kinetic energies smaller than 14 Ry and all atoms were fully relaxed.

Each of the mechanisms discussed below defines a specific path for the diffusing atom(s) to follow. However, the position of a saddle point, unless determined by symmetry, is usually unknown. A point-by-point calculation of the total energy along the trajectory can be costly. As an alternative, we propose a new, more efficient procedure to determine a migration barrier, which we call an “adiabatic trajectory” simulation. The main idea is that the diffusing atom moves with a constant, small speed (e.g., thermal speed at 300 K) along the path defined by the mechanism under consideration, while the remaining atoms continuously relax in response to its motion. As in a CP simulation, the system moves along the lowest energy Born-Oppenheimer surface [7]. The velocity of each of the remaining atoms is decomposed according to the direction of the force acting on it. The component perpendicular to the force is set to zero and the parallel one is reduced by a factor of 3 if it is antiparallel to the force. This procedure removes the excess energy introduced by the constant speed motion of the diffusing atom and leads to a fast relaxation of the whole system. In cases where level crossing occurs, we use the finite temperature CP formalism [11] with $kT=0.1$ eV for stability. Our tests indicate that the adiabatic trajectory simulation is about

4 times faster than a point-by-point evaluation of the total energy, while differing from its results by less than 0.1 eV.

The diffusion of Zn in GaAs is the rate determining step in GaAs/AlAs superlattices, since it has been found that Zn diffuses much slower in GaAs than in AlAs [12]. Therefore, we focus mainly on GaAs. Since both the Zn diffusion and the interdiffusion mechanisms involve native defects, knowledge of their formation energies and concentrations is needed. We computed the formation energies of all tetrahedral point defects: two vacancies V_{Ga} and V_{As} , two antisites As_{Ga} and Ga_{As} , and four tetrahedral interstitials As_{TGa} , As_{TAs} , Ga_{TGa} , and Ga_{TAs} , where the subscripts indicate the nearest-neighbor atoms. As_{TAs} is found to be unstable. It relaxes to form a split $\text{As}_J\text{-Ga}_{\text{Ga}}$ pair, lowering the total energy by 1.9 eV. Very recently, Chadi [13] proposed new split interstitial sites for Ga and As. We find that an $\text{As}_J\text{-As}_{\text{As}}$ pair is 0.2 eV lower than the $\text{As}_J\text{-Ga}_{\text{Ga}}$ pair. For Ga_J^+ , however, a split Ga_J^+ relaxes to the tetrahedral interstitial site.

The concentrations of the native defects were determined using the formalism of Refs. [14] and [15], which assumes equilibrium between GaAs and bulk Ga and As. The difference between the chemical potentials of Ga and As is then constrained to the theoretical heat of formation of GaAs, which is 0.71 eV for our pseudopotentials and cutoffs [16]. (The experimental value is 0.75 eV.) Since GaAs and AlAs are in contact in a superlattice, the value of the chemical potential for As in GaAs and the cohesive energy of AlAs determines the chemical potential of Al. The equilibrium concentration of a defect i is given by $C_i = N_s \exp[-(E_{f,i} - S_{f,i}T)/k_B T]$, where N_s is the concentration of sublattice sites, and $E_{f,i}$ and $S_{f,i}$ are its formation energy and entropy, respectively. An *ab initio* calculation of the formation entropy for all the native defects in GaAs would be prohibitively expensive at present [17]. We thus use a value of $6k_B$ for all the defects, which is the result of a recent extensive calculation for vacancies and interstitials in Si [17]. For charged defects, the well-known inability of local density theory to reproduce semiconductor band gaps leads to an overestimate of their concentrations, but this does not affect the energetic ordering of the various diffusion mechanisms.

The formation energies depend linearly on the chemical potentials of the atomic reservoirs for Zn, Ga, and As, and on the Fermi level. If the stoichiometry deviation in p -type GaAs is smaller than 0.02%, the variation in the effective chemical potentials is restricted to 0.1 eV. The position of the Fermi level is determined by the electrical neutrality condition at a given doping and temperature. It depends thus on the chemical potentials, although this dependence is very weak near the perfect stoichiometry limit. Whenever an explicit value for the temperature is needed, we use 600°C, which is the observed interdiffusion temperature.

In undoped GaAs, the native defects with the lowest

formation energies are Ga_{TAs}^+ ($E_{\text{form}}=1.3$ eV), As_{Ga} ($E_{\text{form}}=1.4$ eV), and $\text{Ga}_{\text{As}}^{2-}$ ($E_{\text{form}}=1.4$ eV). The latter is the main component of the $EL2$ defect [18,19] and is the dominant defect in low temperature GaAs [20]. Since As_{Ga} is not mobile at interdiffusion temperatures, the main contribution to intrinsic interdiffusion should come from the Ga interstitial. The formation energy of V_{Ga}^{3-} , which plays an important role in n -type GaAs, is 2.0 eV. A change in stoichiometry at a 10^{18} cm^{-3} level from As-rich to Ga-rich changes these formation energies by less than 0.05 eV. Therefore, a modest stoichiometric deviation would not change the situation. The Ga interstitial is thus the preferred mobile native defect in the intrinsic and p -type material. n -type GaAs needs also to be considered, since in some experiments the material is n type before Zn in-diffusion. In n -type GaAs the defects with lowest formation energy are As_{Ga}^0 (1.2 eV), $\text{Ga}_{\text{As}}^{2-}$ (1.3 eV), V_{Ga}^{3-} (1.6 eV), and Ga_{TAs}^+ (1.5 eV).

Turning to Zn, it is a well-known Ga-site substitutional acceptor. The calculated formation energy for a Zn acceptor with respect to a GaAs crystal in contact with a bulk Zn reservoir is 1.0 eV. For interstitial Zn it is 1.4 eV. Two mechanisms involving a substitutional-interstitial diffusion path for Zn were proposed [2,3], and a good fit to the experimental diffusion profiles has been achieved assuming either [21,22]. The dissociative mechanism [2] assumes that when GaAs is heavily doped with Zn, a small fraction of Zn becomes interstitial through the process $\text{Zn}_{\text{Ga}} \rightarrow \text{Zn}_I + V_{\text{Ga}}$; see Fig. 1. Since V_{Ga} in the $3-$ charge state has the lowest formation energy, we investigated the process $\text{Zn}_{\text{Ga}} \rightarrow \text{Zn}_I^{2+} + V_{\text{Ga}}^{3-}$ via an adiabatic trajectory simulation. The total energy surface along the $(-1, -1, -1)$ direction is shown in Fig. 2. The activation energy is 4.0 eV.

The kick-out mechanism [3] involves a kick-out by an interstitial Ga of a substitutional Zn to an interstitial site $\text{Zn}_{\text{Ga}} + \text{Ga}_I \rightarrow \text{Zn}_I$; see Fig. 1. The formation energy of a $\text{Zn}_{\text{Ga}}\text{-Ga}_{\text{TAs}}$ pair is only 0.8 eV in nearly stoichiometric GaAs. This is due to Coulombic attraction, since this pair can be formally written as $\text{Zn}_{\text{Ga}}^-\text{-Ga}_{\text{TAs}}^+$. Its binding energy is 0.5 eV. A plot of the total energy along the

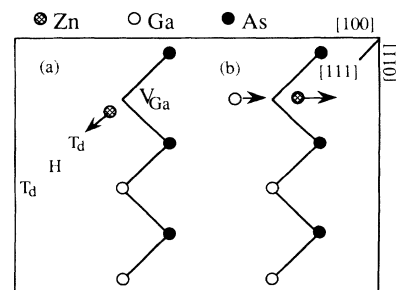


FIG. 1. The two most commonly considered diffusion mechanisms for Zn: (a) dissociative, $\text{Zn}_{\text{Ga}} \rightarrow \text{Zn}_I + V_{\text{Ga}}$ and (b) kick-out, $\text{Ga}_I + \text{Zn}_{\text{Ga}} \rightarrow \text{Zn}_I + \text{Ga}_{\text{Ga}}$; see text.

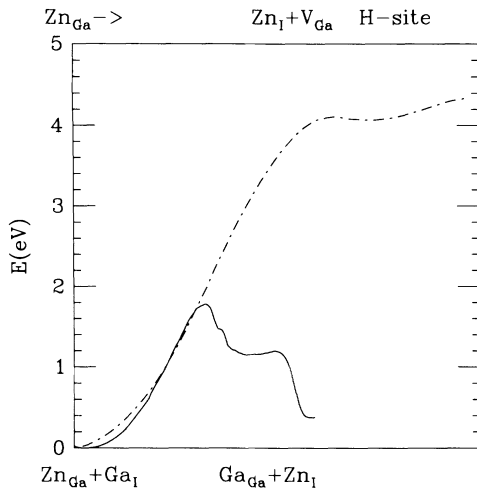


FIG. 2. Total energy for Zn motion along the kick-out path (solid line, bottom scale) and the (100) dissociative path (dashed line, top scale).

(100) adiabatic trajectory, with Ga_{TAs} being the “kicking” atom, gives a barrier of 1.8 eV (see Fig. 2). Following the kick-out, Zn_I can move along the interstitial channel with an activation energy of 0.2 eV or less (depending on the charge state) and then kick-in into another substitutional site. Assuming that the $Zn_{Ga}-Ga_{TAs}$ pair migrates in its initial neutral charge, the activation energy is 2.6 eV.

Another less obvious kick-out, in which a Ga_{TGa} pushes a nearest-neighbor Zn_{Ga} along (111) onto an As site, is also possible [23]. The As atom moves into the interstitial channel, comes around, and pushes Zn along the (1,1,-1) direction onto another Ga site, thereby regenerating the Ga interstitial. In this process, Zn diffuses along the zigzag chain in the (110) plane, with the saddle point occurring when As_I is near the symmetric hexagonal site. The migration and activation energies are 1.9 and 2.7 eV, respectively.

Two V_{As} -based mechanisms have also been proposed [4,5]. Both start with a $Zn_{Ga}-V_{As}$ pair and involve nearest-neighbor or second-nearest-neighbor jumps. In GaAs, the formation energy of the pair is 1.4 eV. We did not investigate the activation barriers of these mechanisms because the total energies of intermediates are above 3.6 and 5.3 eV for the two mechanisms, respectively. A V_{Ga} -based mechanism, in which Zn moves by second-nearest-neighbor jumps is also possible. The formation energy of a $Zn_{Ga}-V_{Ga}$ neutral pair is 3.2 eV and the migration energy is 1.1 eV. The saddle point for this process lies in the (110) plane perpendicular to the plane containing the pair. The formation energy of this pair can be lowered in *n*-type material by supplying additional electrons, but the migration energy would then increase to 1.75 eV.

Comparing all the activation energies, the Ga_I -

mediated kick-out mechanisms have the lowest activation energies for Zn diffusion in GaAs. In the (100) kick-out, the Zn interstitial can move in the interstitial channel with a barrier of only 0.2 eV, while in the (111) kick-out each migration step has to overcome a barrier of 1.9 eV. Therefore, the dominant process is the (100) kick-out mechanism. Its activation energy, 2.6 eV, is in good agreement with the earlier experimental results of 2.5 eV [24] and 2.1–3.1 eV [25].

Since the group-III interstitial kick-out dominates the diffusion in GaAs, we studied only the corresponding processes in AlAs. The migration barriers are 1.2 and 2.0 eV for the (100) and (111) directions, respectively. The (100) kick-out thus dominates in AlAs as well. The lower barrier in AlAs is in good agreement with the experimental data [26].

We now turn to the role of Zn in enhancing the interdiffusion. For interdiffusion to be initiated at 600°C, the concentration of Zn acceptors must exceed 10^{18} [25]. The introduction of each Zn acceptor results in the creation of one group-III interstitial. Therefore, the concentration of group-III interstitials increases dramatically upon Zn in-diffusion. Since the activation energy for the diffusion of interstitial Zn in GaAs is 0.2 eV or less, Zn atoms can penetrate deep into the sample before kicking out a group-III atom. Since the $Zn_{III}-III_I^+$ pairs are bound by Coulomb forces, most of the long-range diffusion must be due to Zn and the interdiffusion should follow the Zn in-diffusion front, which is precisely what is observed experimentally [25].

The remaining task is to compute the activation energies for cation interchange. Note that if Zn is the dominant impurity, the interstitial cations' charge state is +1. We carried out adiabatic trajectory simulations for the (100) kick-out of Ga and Al by the cations: $Al_I^+ + Ga_{Ga} \rightarrow Ga_I^+ + Al_{Ga}$ (in GaAs) and $Ga_I^+ + Al_{Al} \rightarrow Al_I^+ + Ga_{Al}$ (in AlAs). The activation energies are 1.6 and 1.1 eV, respectively. They will vary somewhat during interdiffusion since they depend on the composition of the alloy. Assuming that Zn has already diffused in and the pairs have formed, these are also the activation energies for interdiffusion. The above results thus show that the principal enhancement of the interdiffusion is due to the generation of a large concentration of nonequilibrium cation interstitials through the formation of $Zn_{III}-III$ pairs, rather than to the lowering of the Fermi-level position.

Experimentally, Lee and Laidig [25] observed an average activation energy for interdiffusion of ~ 1 eV in GaAs/AlAs superlattices after the in-diffusion of Zn. Since it is difficult to determine precisely both the onset and the extent of interdiffusion, the agreement between the experimental and theoretical results should be viewed as satisfactory. Yu, Tan, and Gösele [27] have recently confirmed that satisfactory fits to the experimental diffusion profiles for Zn in GaAs can be obtained assum-

ing the dominance of either the dissociative or the kick-out mechanism. They also pointed out that from the two mechanisms only the kick-out mechanism can explain the Zn-induced interdiffusion enhancement. Even if the interdiffusion enhancement is due to the kick-out of Ga interstitials, diffusion of Zn could still involve other mechanisms. For example, photoluminescence from Si- V_{Ga} and V_{As} -Zn complexes was detected in Si-doped GaAs after Zn in-diffusion [28,29]. This finding was interpreted as supportive of the vacancy mechanisms. Indeed, in *n*-type material the present calculations show that the formation energies of V_{Ga}^{\ominus} and Ga_I^+ are almost the same. However, they also show that the activation energies of the vacancy-based mechanisms under interdiffusion conditions are much larger than those of the kick-out mechanism.

In summary, we have used *ab initio* molecular dynamics to study the Zn-enhanced interdiffusion in GaAs/AlAs superlattices. The results provide a microscopic picture of Zn diffusion in GaAs and of the interdiffusion process. The lowest energy diffusion path for substitutional Zn is the (100) kick-out, assisted by group-III interstitials. During Zn in-diffusion, group-III atoms are ejected into the interstitial channel through the kick-out process, providing a nonequilibrium concentration of group-III interstitials. The group-III atoms diffuse rapidly through the interstitial channel and exchange with substitutional group-III atoms, thereby disordering the superlattice.

We are indebted to Dr. C. G. Van de Walle for providing the computed values of cohesive energies of bulk Ga and As. This work is supported by ONR Grant No. N00014-89-J-1827. The calculations have been carried out at the Pittsburgh and North Carolina Supercomputing Centers.

-
- [1] W. D. Laidig, N. Holonyak, Jr., M. D. Camras, K. Hess, J. J. Coleman, P. D. Dapkus, and J. Bardeen, *Appl. Phys. Lett.* **38**, 776 (1981).
 - [2] R. L. Longini, *Solid State Electron.* **5**, 127 (1962).
 - [3] U. Gösele and F. Morehead, *J. Appl. Phys.* **52**, 4617 (1981).
 - [4] D. Shaw, *Phys. Status Solidi (a)* **86**, 629 (1984).
 - [5] J. A. Van Vechten, *J. Phys. C* **17**, L933 (1984).
 - [6] P. Y. Tan and U. Gösele, *J. Appl. Phys.* **61**, 1841 (1987).

- [7] R. Car and M. Parrinello, *Phys. Rev. Lett.* **55**, 2471 (1985).
- [8] G. B. Bachelet, D. R. Hamann, and M. Schlüter, *Phys. Rev. B* **26**, 4199 (1982).
- [9] X. Gonze, R. Stumpf, and M. Scheffler, *Phys. Rev. B* **44**, 8503 (1991).
- [10] The lattice constants of ZnSe and ZnTe are reproduced within 2% by the soft Zn potential, but the bulk moduli are significantly affected. The inclusion of the 3*d* shell in the core might have led to a slight underestimate of the diffusion barriers in GaAs/AlAs. See also S.-H. Wei and Alex Zunger, *Phys. Rev. B* **37**, 8958 (1988).
- [11] M. P. Grumbach, D. Hohl, R. M. Martin, and R. Car, *Bull. Am. Phys. Soc.* **36**, 836 (1991).
- [12] The dependence of Zn diffusion on Al content was investigated in the ternary system $\text{Al}_x\text{Ga}_{1-x}\text{As}$ in Ref. [26]. If the experimental data are extrapolated to $x=1$, the diffusion of Zn in AlAs should be about 10 times faster than in GaAs.
- [13] D. J. Chadi (to be published).
- [14] D. B. Laks, C. G. Van de Walle, G. F. Neumark, and S. T. Pantelides, *Phys. Rev. Lett.* **66**, 648 (1991).
- [15] S. B. Zhang and John E. Northrup, *Phys. Rev. Lett.* **67**, 2339 (1991).
- [16] C. G. Van de Walle (unpublished).
- [17] R. Car, P. Blöchl, and E. Smargiassi, *Mater. Sci. Forum* **83-87**, 433 (1991).
- [18] J. Dabrowski and M. Scheffler, *Phys. Rev. Lett.* **60**, 2183 (1988).
- [19] D. J. Chadi and K. J. Chang, *Phys. Rev. Lett.* **60**, 2187 (1988).
- [20] M. Kaminska and E. R. Weber, *Mater. Sci. Forum* **83-87**, 1033 (1992).
- [21] A. H. van Ommen, *J. Appl. Phys.* **54**, 5055 (1983).
- [22] K. B. Kahen, *Appl. Phys. Lett.* **55**, 2117 (1989).
- [23] C. S. Nichols, C. G. Van de Walle, and S. T. Pantelides, *Phys. Rev. B* **40**, 5484 (1989).
- [24] B. Goldstein, *Phys. Rev.* **118**, 1024 (1960).
- [25] J. W. Lee and W. D. Laidig, *J. Electron. Mater.* **13**, 147 (1984).
- [26] C. P. Lee, S. Margalit, and A. Yariv, *Solid State Electron.* **21**, 905 (1978).
- [27] S. Yu, T. Y. Tan, and U. Gösele, *J. Appl. Phys.* **69**, 3547 (1991).
- [28] N. H. Ky, L. Pavesi, D. Araújo, J. D. Ganière, and F. K. Reinhart, *J. Appl. Phys.* **69**, 7585 (1991).
- [29] L. Pavesi, D. Araújo, N. H. Ky, J. D. Ganière, F. K. Reinhart, and P. A. Buffat, *Opt. Quantum Electron.* **23**, S789 (1991).